Molecular Catalysis 497 (2020) 111220

Contents lists available at ScienceDirect

Molecular Catalysis

journal homepage: www.journals.elsevier.com/molecular-catalysis

Tetranuclear Zn complex covalently immobilized on sulfopropylsilylated mesoporous silica: An efficient catalyst for ring opening reaction of epoxide with amine

Divya Jadav [a], Pooja Shukla [a], Rajib Bandyopadhyay [b], Yoshihiro Kubota [c], Sourav Das [a,*], Mahuya Bandyopadhyay [a,*]

[a] Institute of Infrastructure, Technology, Research and Management, IITRAM, Maninagar, Ahmedabad, Gujarat, India
[b] School of Technology, Pandit Deendayal Petroleum University, Raisan, Gandhinagar, Gujarat, India
[c] Department of Material Science & Chemical Engineering, Yokohama National University, Yokohama, Japan

ARTICLE INFO

Keywords:
Tetranuclear Zn complex
Mesoporous silica
Ring opening reaction
β-Aminoalcohols

ABSTRACT

Tetranuclear Zn complex, $[Zn_4(L)_2(LH)_2((CH_3)_2SO)_2]\cdot 2CH_3OH\cdot(CH_3)_2SO\cdot H_2O$ (**1**) [where LH_3 = 3-(*E*)-(2-hydroxyphenylimino)methyl-4-hydroxy-5-hydroxymethylphenyl (LH_3)] was prepared and characterized by single-crystal X-ray analysis. Then, it was incorporated to the sulfopropylsilylated MCM-48, MCM-41 and SBA-15 mesoporous silica materials. The prepared materials were thoroughly characterized by XRD, FT-IR, N_2 adsorption/desorption analysis, NH_3-TPD, TGA, SEM-EDX and ICP-OES measurements. These catalysts were successfully used for the ring opening reaction of propylene oxide with morpholine producing the corresponding β-aminoalcohols. An abrupt increase in catalytic activities was observed after anchoring of the tetranuclear Zn complex onto the inner surface of sulfopropylsilylated mesoporous materials. Among all the catalysts, the tetranuclear Zn complex incorporated MCM-48 was found to be most active in this reaction system and gave maximum 95% conversion. Catalysis by the tetranuclear Zn complex immobilized on MCM-48 was totally heterogeneous and the catalyst was recyclable up to 4 times without leaching.

Introduction

Transition metal complexes are quite popular in the oxidation/reduction of organic substrates and for the synthesis of fine chemicals, but some disadvantages related to their use, such as difficult recovery from the reaction mixture, low stability, high cost, limits their use, especially from an industrial point of view. Their immobilisation on solid supports leads to an important class of organic inorganic hybrid materials with certain added advantages like selectivity, easy separation from the reaction mixture and recycle capability [1–4]. These immobilized materials can be utilized to develop new environment friendly technologies.

Influence of zinc complexes arises from its excellent Lewis acidity, rapid ligand exchange, being non-toxic and non-redox active making it most obvious choice in catalytic studies. In order to deeply understand these traits, one should understand and appreciate how the chemistry of Zn^{2+} is influenced by its coordination sphere. Reported metal ion systems in most cases have Schiff- based ligands that are tridentate or tetradentate in nature providing necessary free coordination sites. It facilitates the formation of such complex which efficiently allows us to study the role of multidentate ligands, geometry, labile groups as well as its efficacy in the catalytic activity of the desired systems [5]. In case of epoxide ring opening reaction, zinc complexes are effective in inducing 'electrophilic activation' of the epoxide ring. Besides, the strong electrophilicity of the Zn^{2+} ion delocalized the negative charge of the oxygen atom in the transition state of the epoxide ring opening reaction and assisted the progress of the reversible reaction in the forward direction. Basically, Zn^{2+} containing metal complexes due their flexibility in coordination sites can play a delicate role in counterbalance between Lewis acid and electrostatic activation of the substrate [6]. Sometimes, substrate can be cooperatively activated by dual metal components present in the polynuclear metal complexes [7,8].

Till now, a wide varieties of hybrid solid supports have been used, namely "bulk'' supports including mesoporous silicas, carbon materials, clay based materials and metal–organic frameworks or "nano-supports'' like nano-silicas, carbon nano-tubes, magnetic iron oxide nano-particles,

* Corresponding authors.
E-mail addresses: souravdas@iitram.ac.in (S. Das), mahuyabandyopadhyay@iitram.ac.in (M. Bandyopadhyay).

https://doi.org/10.1016/j.mcat.2020.111220
Received 30 July 2020; Received in revised form 6 September 2020; Accepted 7 September 2020
Available online 1 October 2020

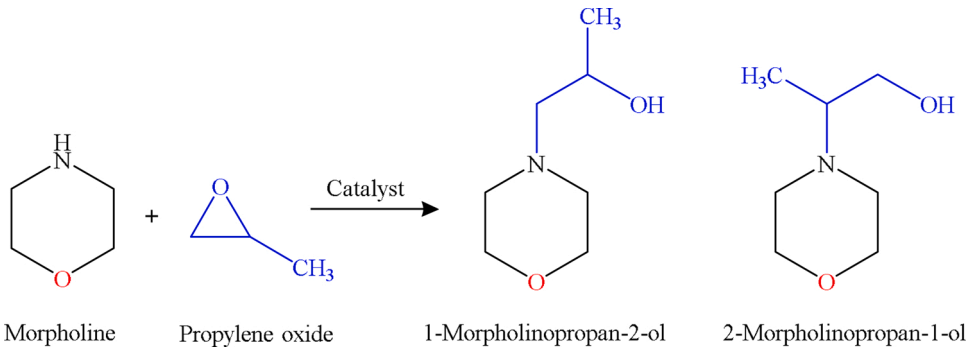

Scheme 1. Ring opening reaction of propylene oxide with morpholine.

etc. [9]. The promising properties of high surface area, narrow pore size distribution and flexible pore diameters (>2 nm) of ordered mesoporous materials have attracted enough consideration for their potential applications in adsorption, separation, tailored delivery devices for bio-applications, chemical sensing and catalysis. In acid catalyzed reactions like alkylation, acylation, esterification, biodiesel production to redox reaction such as oxidation of alcohols, alkenes, sulfides and hydrogenation of acids, aldehydes and ketones and alkenes/alkynes also including asymmetric applications, such materials have been extensively used [10–19].

The combination of Schiff based complexes with functionalized porous materials can be a promising approach towards the industrially important catalytic reactions. S. Sharma et al. [20] synthesized high order of dioxygen binding to the immobilized Co^{II} complexes in porous materials (90% for P-1. py[Co^{II}]) and used them as heterogeneous oxidation catalysts for substituted phenol. There are reports on aminopropyl-functionalized SBA-15, as a support for anchoring tri (8-quinolinolato) iron complexes [21] and mono- and polynuclear carbonyl compounds of Rh, Ir, encapsulated and different oxovanadium and other metal complexes in the super cages of Y zeolites [22–28]. As reported, oxovanadium(IV) and copper(II) complexes are more stable as dimmer [29–32]; the zeolitic pore allows them to exist as stable monomeric active center by preventing dimerization. There are also other reports on synthesis and catalytic properties of Cu (II) complex modified MCM-41 material in variety of chemical conversions [33–35].

Epoxides are significant class of synthons which has profound use in synthetic organic chemistry [36–38]. Epoxide ring opening reactions lead to the formation of industrially important multipurpose products. The presence of nucleophiles, such as amines, ammonia, alcohols, phenols, water, thiols, etc. is required for this reaction to attack the substrate. Ring opening of epoxide by amine yields β-amino alcohols (Scheme 1) which are industrially important for the production of biologically active natural/unnatural materials and also can be used as a chiral ligand in asymmetric synthesis [39–42]. β-amino alcohols can also be used as a potential inhibitor of the anti-tubercular target N-acetyltransferase [43]. Traditionally the epoxide ring opening reactions are carried out at elevated temperature, however, at higher temperature the formation of unwanted side reactions [44] cannot be avoided. In most of the cases, weak nucleophile reacts slowly and yields low regioselective products. Some reported studies demonstrate the use of excess amount of sulfamic acid, modified montmorillonite clay, mesoporous carbon, ionic liquid, cobalt(II) chloride, polymeric rare earth complexes, nanoporous aluminosilicate and Lewis acid as a catalyst in epoxide ring opening reaction performed at elevated temperature, high pressure and long reaction time [45–52]. Henceforth, developing a method which will work at mild condition is always an effort for the scientific fraternity. Researchers are already working in this area to achieve higher yield at mild and solvent free reaction system [53–57].

Inspired by the versatile application of metal complex incorporated porous silica materials as a catalyst in different industrially important chemical reactions, we have prepared new tetranuclear open-cubane shaped Zn complex and it was anchored to the sulfopropylsilylated mesoporous silica supports (MCM-48, MCM-41 and SBA-15). Owing to high surface area which offers effective number of active sites than non-crystalline amorphous silica [58,59], mesoporous crystalline materials are preferred as a support for functionalization. The prepared materials were thoroughly characterized using different physicochemical characterization techniques to have a clear image of the successful anchoring of Zn complex in mesoporous silica support. In our present work, we have synthesized and used tetranuclear Zn-complex to incorporate in sulfonic acid functionalized mesoporous silica and explored their catalytic activities in epoxide ring opening reaction.

Experimental

Synthesis and preparation of sulfopropylsilylated MCM-48, MCM-41 and SBA-15

Mesoporous MCM-48, MCM-41 and SBA-15 materials were synthesized as per the conditions mentioned in the literature [60]. MCM-48, MCM-41 and SBA-15 materials were synthesized using molar gel composition of 1.0 TEOS:0.7 CTACl:0.5 NaOH:64 H_2O, 1.0 TEOS:0.12 CTABr:0.23 NaOH:130 H_2O and 1.0 TEOS:0.017 Pluronic123:6.1 HCl:165 H_2O respectively. The as-made materials were calcined at 550 °C for 5 h.

Post-synthetic modification was carried out by using 3-mercaptopropyltrimethoxysilane (MPTES) using literature procedure by our group [61]. Appropriate amount of catalyst was vacuum dried and refluxed at 110 °C for 12 h with excess of MPTES. The solid material was recovered and oxidation of thiol group was done by using excess of 30% H_2O_2 solution for 24 h followed by acidification with excess of 0.2 M H_2SO_4. Finally, the solid powder was filtered off, washed with water, dried at 60 °C. The schematic diagram for the functionalization process is explained in Scheme 3.

Synthetic procedure for the preparation of complex

The ligand (*E*)-2-(hydroxymethyl)-6-(((2-hydroxyphenyl) imino) methyl)-4-methylphenol (LH_3) was prepared from a known procedure [62]. Zinc acetate dihydrate as well as 2-aminophenol were received from Sigma Aldrich, India and were used as such. The base tetra butyl ammonium hydroxide (TBA-OH) was obtained from SRL Chemicals, India. The other reagents were purchased from commercial sources and utilized without any further purification. Complex was prepared by using above mentioned ligand and the procedure is described as below.

$$[Zn_4(L)_2(LH)_2((CH_3)_2SO)_2]\cdot 2CH_3OH\cdot(CH_3)_2SO\cdot H_2O \quad (1)$$

Ligand LH_3 (0.041 gm, 0.1593 mmoles) was dissolved in methanol and after stirring for fifteen minutes, $Zn(OAc)_2\cdot 2H_2O$ (0.0073 gm, 0.0398 mmoles) was added. To it three moles of TBA-OH was added

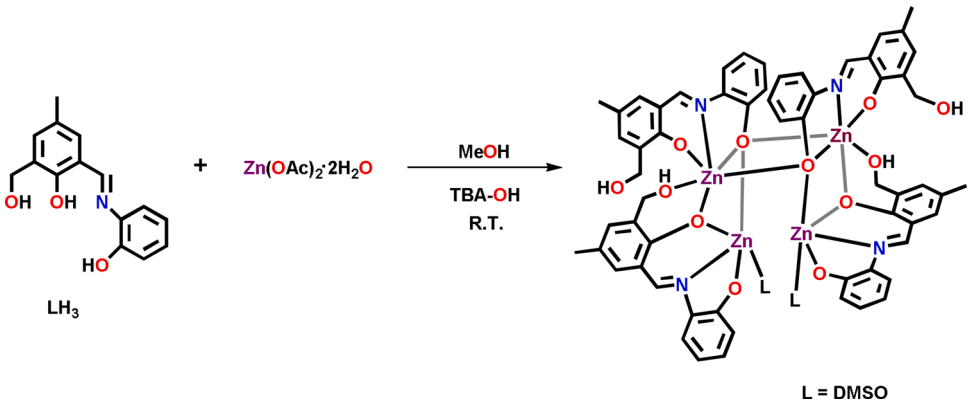

Scheme 2. Synthesis of the homometallic Zn_4 complex (**1**).

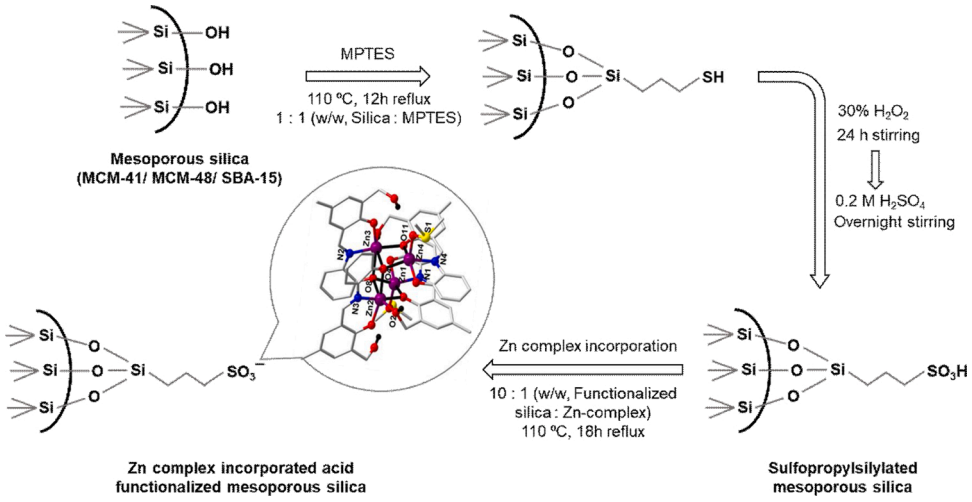

Scheme 3. Preparation of Zn complex incorporated sulfopropylsilylated mesoporous silica.

giving yellow colored precipitate immediately. After stirring for twelve hours, the solution was evaporated in vacuum and dissolved in DMSO and dichloroform. One week later, yellow colored crystals suitable for single crystal X-ray diffraction were obtained (Scheme 2). Yield: 0.034gm, 53.01% (based on Zn). Anal. Calcd. $C_{68}H_{79}N_4O_{18}S_3Zn_4$ (1597.91): C, 43.12; H, 5.59; N, 4.44. Found: C, 42.98; H, 4.05; N, 5.60.

Zn complex incorporation to the mesoporous silica

Sulfopropylsilylated mesoporous silica was used as a host to immobilize tetranuclear cubane shaped Zn complex to prepare the organic-inorganic hybrid materials (Scheme 3). Prior to the anchoring, 400 mg of sulfopropylsilylated mesoporous silica was dried at 80 °C for 3 h and then 40 mg of Zn complex was mixed with it in dry toluene followed by refluxing at 110 °C for 18 h. The solid product was then recovered by filtration, washed thoroughly with toluene and dried at 80 °C for 12 h. Zn complex incorporated MCM-48, MCM-41 and SBA-15 materials were denoted as M-48-S-Zn, M-41-S-Zn and S-15-S-Zn respectively.

Characterization

The crystallinity and phase purity of the prepared materials were investigated by powder X-ray diffraction (XRD; Ultima-IV, Rigaku) via Cu Kα radiation at 40 kV and 20 mA. Nitrogen (–196 °C) adsorption-desorption isotherm analysis was performed on BELMAX, MicrotracBEL instrument measured for samples pre-treated at 150 °C for 4 h. Thermogravimetric analysis (TGA) was performed on a Thermo plus EVO II TG 8120 (Rigaku) instrument. The sample was heated from room temperature to 800 °C at 10 °C min^{-1} in a dry air flow of 30 mL min^{-1}. The temperature programme desorption (NH_3-TPD) was carried out with a chemisorption analyzer (BELCAT-B, MicrotracBEL) and a thermal conductivity detector (TCD). The fresh sample (50 mg) was preheated at 600 °C for 1 h prior to measurement under He flow at 50 cm^3 (NTP) min^{-1} and then it was cooled before being exposed to ammonia. NH_3 adsorption was performed at 100 °C using 5% NH_3/He flow at 50 cm^3 (NTP) min^{-1}, and the TPD profiles were collected by increasing the temperature range from 100-500 °C at a ramp rate of 10 °C min^{-1} under a He flow at 30 cm^3 (NTP) min^{-1}. Total number of acid sites was determined from the area of the h-peak [63] in the TPD profiles. The Si/Zn molar ratios were measured by inductively coupled plasma-atomic emission spectroscopy (ICP-AES; ICPE-9000, Shimadzu). The FT-IR spectroscopic analysis (PerkinElmer, Spectrum Two) was performed to evident the successful grafting of Zn complex to the mesoporous supports. The IR spectra was recorded at room temperature at resolution of 2 cm^{-1} in the range of 500–4000 cm^{-1} with the diamond crystal. The morphological study and elemental analysis of the zeolite catalysts were performed by Field Emission Scanning Electron Microscopy (FE-SEM with EDX; JSM-7600 F, JEOL). Elemental analysis was measured using Thermoquest CE instrument CHNS-O, EA/110 model. NMR spectra with $CDCl_3$ solutions were performed by a JEOL JNM LAMBDA 400 model spectrometer operating at 400 MHz.

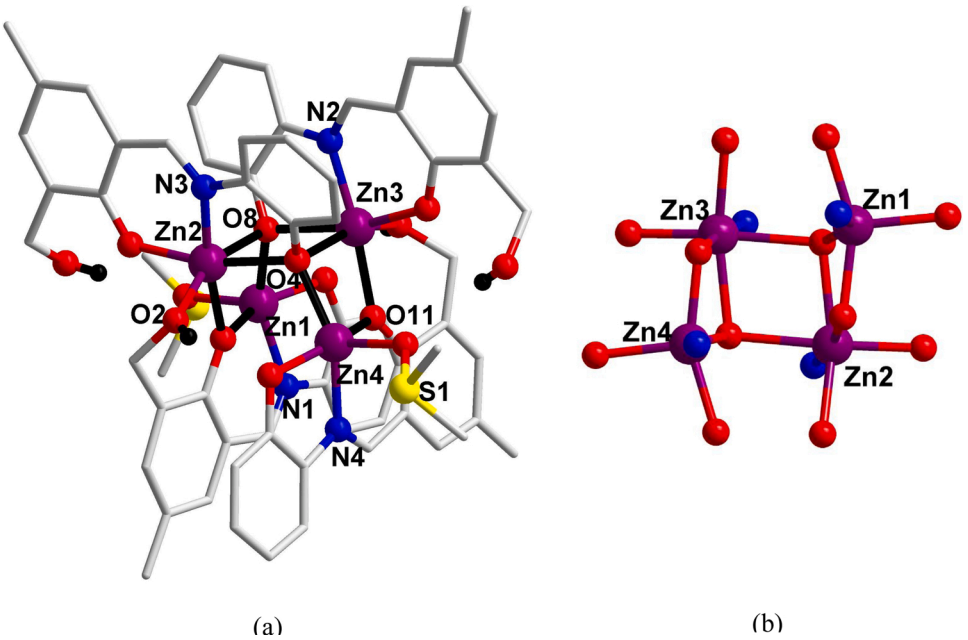

Fig. 1. (a). Molecular structure of complex **1** (Hydrogen atoms except those of protonated ligand are omitted for clarity). **(b)** Coordination framework of **1** displaying open half cubane like structure. Selected bond distance (Å) and bond angle (°) parameters: Zn(1) - O(2) = 2.015 (5), Zn(1)- O(1) = 2.009(5), Zn(1)- O(4) = 2.037(5), Zn(1)- N(1) = 2.056(7), Zn(1) - O(14) = 2.053(6), Zn(2) – N(3) = 2.023(6), Zn(2) – O (4) = 2.244(5), Zn(2) – O(7) = 1.994(6), Zn(2) – O(8) = 2.259(5),), Zn(2) – O(2) = 2.089(5), Zn(2) – O(3) = 2.101(6), Zn(3) – O(4) = 2.259 (5), Zn(3) – O(8) = 2.222(5), Zn(3) – O(11) = 2.082(5), Zn(3) – O(5) = 2.010(6), Zn(3) – O (12) = 2.112(5), Zn(3) – N(2) = 2.031(6), Zn(4) – O(10) = 2.013(5), Zn(4) – N(4) = 2.058(7), Zn(4) – O(13) = 2.052(6), Zn(4)-O(11) = 2.017 (5), Zn(4) – O(8) = 2.047(5). Zn(1) – O(4) – Zn (2) = 95.1(2), Zn(1) –O(2) – Zn(2) = 100.8(2), Zn(1) – O(4) – Zn(3) = 111.2(2), Zn(2) – O(4) – Zn(3) = 100.5(2), Zn(3) – O(8) – Zn(2) = 101.18(19), Zn(4) – O(8) – Zn(2) = 110.9(2), Zn(4) – O(8) – Zn(3) = 95.8(2), Zn(4) – O(11) – Zn(3) = 101.2(2).

X-ray crystallography

Crystallographic data for the **1** were collected with a Bruker Apex II CCD diffractometer with graphite monochromated Mo-Kα radiation (λ =0.71073 Å). Data processing was completed with the help of SMART [64] and SAINT [64] processing program. *SADABS* [65] was used for absorption correction, and SHELXTL [65,66] was used for space group, structure determination and least-squares refinements on *F2*. The crystal structures were solved and refined by full-matrix least-squares methods against *F2* by using the program *SHELXL-2014* [67] and *Olex-2* [68] software. The hydrogen atoms were set at calculated positions and refined with the help of riding model. The non-hydrogen atoms present in the complex were refined by anisotropic displacement parameters. *Diamond 3.1e* [69] was used to obtain the crystallographic structures. The solvent accessible voids present in **1** were assumed to be filled with certain disordered molecules of both methanol and DMSO which were unable to be modeled. Utilizing "PLATON/ "SQUEEZE" [70,71] program to remove those disordered solvent molecules (complex **1**, $2CH_3OH$, $1(CH_3)_2SO$), $1H_2O$). Total solvent-accessible void is of volume is 743 $Å^3$ (per unit cell) which coincides to total electron count removed to 171 per unit cell. The total electron removed are 85 electrons per molecule (Z = 2). The crystal data can be acquired from the Cambridge Crystallographic Data Centre free of cost as CCDC 2002850 (**1**) from www.ccdc.cam.ac.uk/data_request/cif. Details of crystallographic data and structure refinement parameters are given in Table S1.

Catalytic reaction

Epoxide ring opening reaction of propylene oxide with morpholine was performed under solvent free condition using a series of prepared Zn complex grafted sulfopropylsilylated mesoporous materials. For a typical reaction procedure, required amount of catalyst was activated at 80 °C for 1 h. Propylene oxide, morpholine and catalyst were taken in a round bottom flask and the reaction mixture was allowed to stir at 70 °C using reflux condenser. The catalyst was filtered off from the resulting liquid and the liquid was subjected to Gas chromatographic analysis (Thermo Fisher Trace-1310, TG 5 column). A series of reactions were performed to optimize the reaction parameters to maximize the reactant conversion. The products were identified by means of GCMS (Perkin Elmer Clarus 500) using DB-5 MS Ui Column (30 m-long, 0.25 μm thickness and 0.25 mm-i.d.). Mass fragment of the products (around 145 *m/z*) were observed in GC–MS analysis which clearly confirm the formation of regioisomer products (1-Morpholinopropan-2-ol and 2-Morpholinopropan-1-ol). After removal of catalyst, reaction filtrate was further characterized by ^1H NMR and mixture of both the regioisomers were observed in the data.

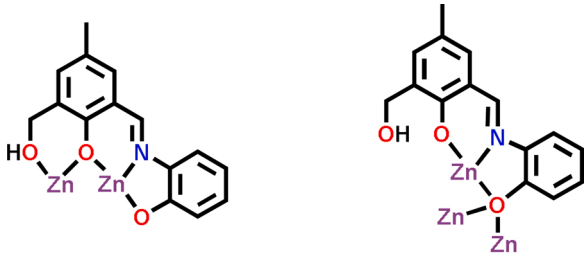

μ_2-η^1:η^1:η^2:η^1 μ_3-η^3:η^1:η^1

Scheme 4. Two different binding mode of ligands $[LH]^{2-}$ for Zn(II) ions.

Results and discussion

X-Ray crystal structure $[Zn_4(l)_2(LH)_2((CH_3)_2SO)_2]\cdot 2CH_3OH\cdot (CH_3)_2SO\cdot H_2O$ (1)

Single crystal X-ray diffraction analysis reveals that homometallic tetranuclear complex **1** crystallizes in the triclinic system with *P*-1 space group (Z = 2). A perceptive view of the molecular structure of **1** is displayed in Fig. 1a. Bond parameters associated with **1** are given in the caption of Fig. 1. The structural analysis of **1** imparts that the crystallographic independent unit contains one tetranuclear unit, $[Zn(LH)_4((CH_3)_2SO)_2]$. Molecular complex of **1** comprises a double open-cubane type $[Zn_4(\mu_3\text{-}O)_2(\mu_2\text{-}O)_2]^{4+}$ core which is constructed by four di-deprotonated Schiff base ligands $[HL^{2-}]$. Here it is noteworthy to mention that in terms of binding capability two pairs of nonequivalent ligands $[HL^{2-}]$ are present in the system. Each ligand from a pair, chelates two Zn(II) ions via utilizing its all potential binding mode in μ_2-η^1:η^1:η^2:η^1-O, N, O, O fashion, while other ligand form a different pair

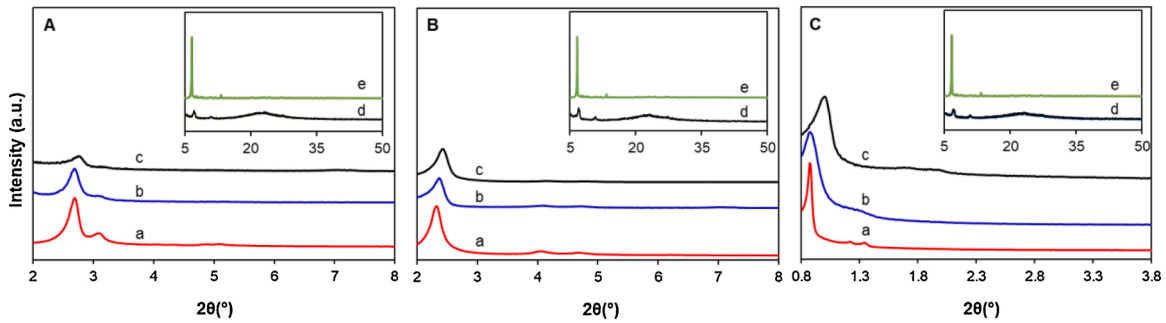

Fig. 2. Powder XRD patterns of (a) calcined, (b) sulfopropylsilylated, (c) Zn complex incorporated materials, (d) high angle XRD pattern of Zn complex incorporated materials and (e) pure Zn complex: (A) MCM-48, (B) MCM-41 and (C) SBA-15.

accommodates three Zn(II) ions utilizing its partial coordination binding in μ_3-η^3: η^1: η^1-O, N, O mode (Scheme 4). Fig. 1b unveils a simplified layout of coordination environment around the four Zn(II) ions. The overall structure of **1** contains two structurally distinct Zn(II) ions. The metal ions, Zn1 and Zn4 are five-coordinate and shows similar square pyramidal geometry, while the other two metal centres, Zn2 and Zn3 are present in a distorted octahedral geometry. The Addison distortion [72] indexes of Zn1 and Zn4 are found to be τ_{Zn1} = 0.1394 and τ_{Zn4} = 0.10435, respectively which further indicates that Zn1 and Zn4 centres possess distorted square pyramidal geometries. The basal planes of the square pyramid ligated by one imine nitrogen and two phenoxide oxygen atoms of the partially deprotonated ligand $[HL]^{2-}$ and the μ_3-phenoxido oxygen atom of another deprotonated ligand $[HL]^{2-}$.

The apical position of the square pyramid is occupied by dimethyl sulphoxide molecule. The basal bond lengths of the square pyramid are in the range of 2.006(5) Å to 2.057(7) Å and the average apical bond distance is 2.055 Å. On the other hand, Zn2 and Zn3 centres adopt distorted octahedron geometry where basal plane is achieved by the imine nitrogen, phenoxido, μ_3-phenoxido oxygen atoms of one HL^{2-} ligand and μ_2-phenoxido oxygen atoms from another HL^{2-} ligand, and one of the axial position is occupied by oxygen atoms from the benzyl alcohol groups from later ligand and other axial position is occupied by μ_3-phenoxido oxygen atoms of another HL^{2-} ligand (Fig. S1). The equatorial bond distances vary from 1.993(6) – 2.260(4) Å, while the axial bond lengths fall in the range from 2.023(6) – 2.087(5) Å. Collected coordination action of all four HL^{2-} ligands form a open-cubane type $[Zn_4(\mu_3\text{-}O)_2(\mu_2\text{-}O)_2]^{4+}$ core where, the corners of the cubane are occupied by Zn(II) atoms and bridging phenoxy O atoms. Zn····Zn distances within Zn_4O_4 cubane cores are different and are in the range of 2.018(5) to 2.260(4) while the average bond angle of Zn-O-Zn is 106.01°. The average bond angle of Zn-O-Zn and Zn····Zn distances within Zn_4O_4 cubane cores is almost comparable with the reported ones [73,74].

Structural Integrity studies by characterization

The powder XRD patterns of unmodified and modified materials are depicted in Fig. 2, high angle XRD patterns are shown in the inset of each of the figures. Low angle diffraction patterns of MCM-48, MCM-41 and SBA-15 show well resolved characteristic reflections revealing pure mesoporous phase. In systematic studies of mesoporous/sorbate system it is already proved that with the tethering of the functional groups into the pores and surface of the host molecules decreases the peak intensity in the diffraction patters [75]. The higher the electron density of the sorbate molecules the lower the peak intensity, however, the successive anchoring of the molecules restores the scattering contrast leading to the

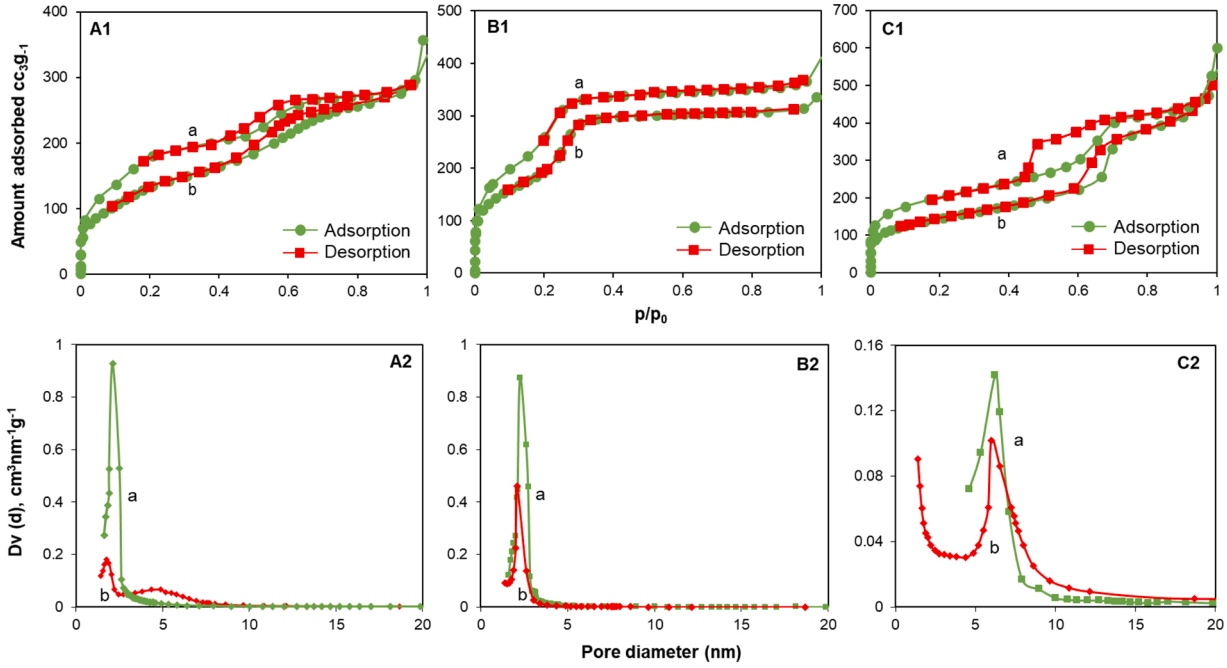

Fig. 3. N_2 adsorption/desorption isotherm of (a) sulfonic acid functionalized, (b) Zn complex incorporated (A1) MCM-48, (B1) MCM-41 and (C1) SBA-15 materials. Pore size distribution curve of (a) sulfonic acid functionalized (b) Zn complex incorporated (A2) MCM-48, (B2) MCM-41 and (C2) SBA-15 materials.

Table 1
Characteristics of various unmodified and modified mesoporous materials

Catalyst	Surface area[a] (m^2/g)	Pore volume[b] (cc/g)	Pore diameter[b] (nm)	Si/Zn ratio[c]	Acid concentration (mmol/g)[d]
MCM-48	1351	1.1	2.3	–	–
MCM-48-SO_3H	590	0.44	2.1	–	0.61
MCM-48-SO_3H-Zn	515	0.43	1.7	18.3	0.824
MCM-41	1088	0.99	2.5	–	–
MCM-41-SO_3H	850	0.62	2.3	–	0.3
MCM-41-SO_3H-Zn	715	0.51	2.0	10.6	0.373
SBA-15	852	0.96	6.4	–	–
SBA-15-SO_3H	661	0.85	6.2	–	0.33
SBA-15-SO_3H-Zn	512	0.77	6	17.6	0.33

[a]determined by the BET method, [b]determined by the BJH method, [c]from ICP-OES analysis, and [d]calculated from NH_3-TPD measurement.

diffraction properties of the starting materials again showing the intact mesoporous silica framework after sulfone as well as Zn_4 complex modifications consecutively. The scattering contrast and the resolution of the X-ray powder diagram was reduced in each functionalization step directly proves the successful grafting of the sulfonic acid onto the surface of mesoporous silica by surface silanolic −OH groups followed by covalently linked of Zn-complex with –SO_3H groups.

In order to check the Zn peaks in the mesoporous silica materials due to anchoring of the Zn-complex, high angle X-ray diffraction analysis was also recorded upto 50 °2θ, and compared with pure Zn complex to confirm the anchoring of Zn complex into mesoporous silica, which are shown in the inset of respective figures. All the modified materials showed peak at around 7.7 °2θ which is well matched with the pattern of pure Zn complex, with slight shift of °2θ value of Zn modified samples towards right angle which may be attributed to the change of chemical composition of the Zn complex after covalently linked with –SO_3H groups in mesoporous materials. This observation confirms the presence of Zn complex in modified porous materials without any degradation. This fact was further confirmed by IR, EDX and ICP analyses also and explained in the later sections.

N_2 adsorption/desorption isotherms of MCM-48, MCM-41 and SBA-15 are shown in Fig. 3. The adsorption/desorption isotherms of Zn complex incorporated mesoporous silica are compared with sulfopropylsilylated mesoporous silicas. All the isotherms are of type IV with steep increase around p/p_0 0.3, which is more prominent in case of all the calcined materials (not shown here) and for functionalized MCM-41 and SBA-15 (Fig. 3 B & C), not very sharp for MCM-48 catalyst. The presence of mesopore assembly is confirmed by a sharp increase of adsorbed gas volume due to capillary condensation in a partial pressure of nitrogen ranging between p/p_0 0.1 and 0.8, indicative of narrow and undeviating pore size distribution [60,76–80], which is likely for mesopores. The pore size distribution curve (Fig. 3) of acid modified and acid and Zn modified material was obtained from Barrett-Joyner-Halenda (BJH) method. The reduction of specific surface area, average pore diameter and pore volume were observed for all the samples may be due to the pore filling by tethering of the functionalized materials [81] and are summarized in Table 1. The deterioration of the sharpness in the isotherm of functionalized MCM-48 materials may be due to the decrease of uniformity of the structure after the acid and Zn-complex modifications. Results clearly indicate that Zn complex covalently tethered to the external and internal pore surfaces of all three materials, which was further confirmed by other physico-chemical characterizations.

SEM images of all three modified materials reveal that there was no apparent change in morphology of the materials observed after Zn complex immobilization into the mesoporous materials. Fig. 4 Shows the SEM image of M-48-S-Zn was found in spherical morphology with particle size of approx. 200 nm (0.2 μm).

There were no significant changes in the morphology of M-41-S-Zn and S-15-S-Zn as well (not shown here) show the intactness of the structure even after modification. SEM-EDX analysis of a selected area of Zn complex modified sulfopropylsilylated MCM-48 material is shown in Fig. 4 B. The peaks of S, Si and Zn elements in the sample is clearly visible here. There is a clear Zn signal at 8.7 Kev for ZnKα. Apart from this the signals for ZnLα and ZnK_β are also present. These results indicate that Zn complex is covalently linked with the –SO_3H group anchored in the mesoporous materials. From the EDX analyses the wt % of Zn present in the materials were calculated. M-48-S-Zn material showed 3.70% of Zn metal in the material whereas M-41-S-Zn and S-15-S-Zn showed 2.31 and 3.35% respectively. These estimations are done to have a rough calculations of bulk elements present in the materials or to confirm the presence of Zn or S in the hybrid materials. We have also used ICP analyses to calculate the exact amount of Zn and S present in the modified materials.

ICP-OES results are summarized in Table 1. Result showed that highest Si/Zn ratio of 18.3 was in M-48-S-Zn with compare to M-41-S-Zn (10.6) and S-15-S-Zn (17.6) materials. 3D structure of MCM-48 material

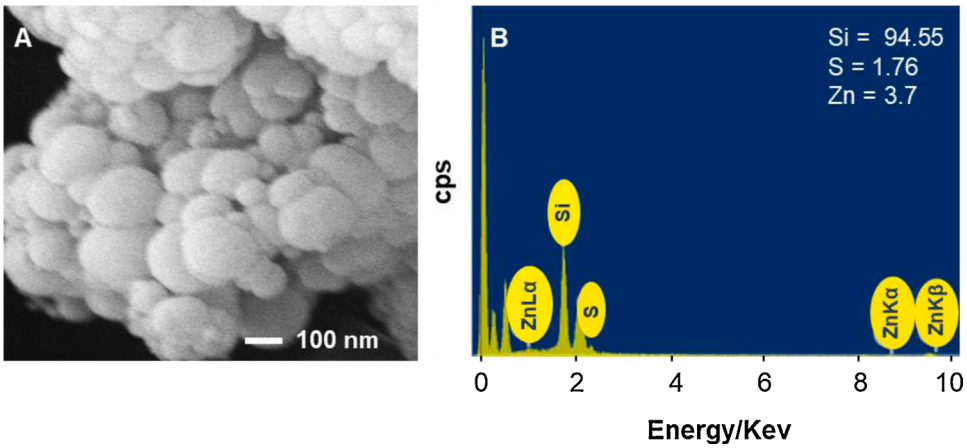

Fig. 4. (A) FE-SEM image and (B) EDX analysis of M-48-S-Zn material.

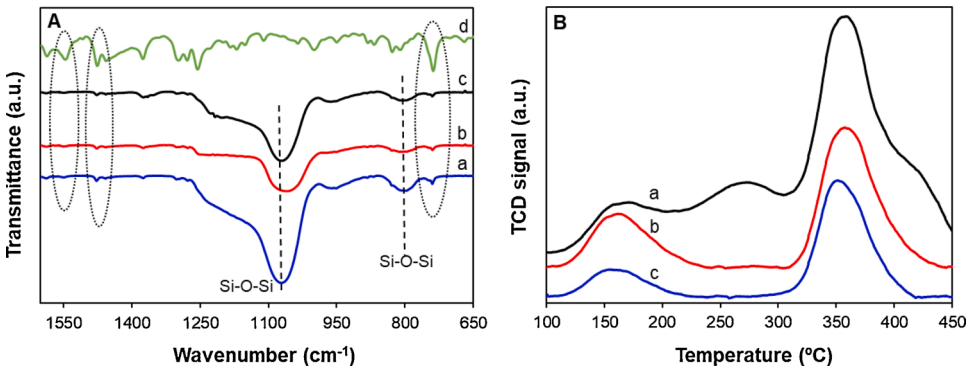

Fig. 5. (A) FT-IR spectra of (a) M-48-S-Zn, (b) M-41-S-Zn, (c) S-15-S-Zn and (d) pure Zn complex. (B) NH_3-TPD profile of (a) M-48-S-Zn, (b) M-41-S-Zn and (c) S-15-S-Zn.

Table 2
TOF, acidity and morpholine conversion with different catalyst amount.

Catalyst	Catalyst amount (mg)	Morpholine conversion (%)	Acid concentration[a] (mmol/g)	TOF (h^{-1})
M-48-S-Zn	5	65	0.824	263
	10	84		170
	20	95		96
M-41-S-Zn	5	58	0.373	519
	10	77		344
	20	86		192
S-15-S-Zn	5	52	0.330	525
	10	64		323
	20	78		197

[a]Calculated from NH_3-TPD measurements.

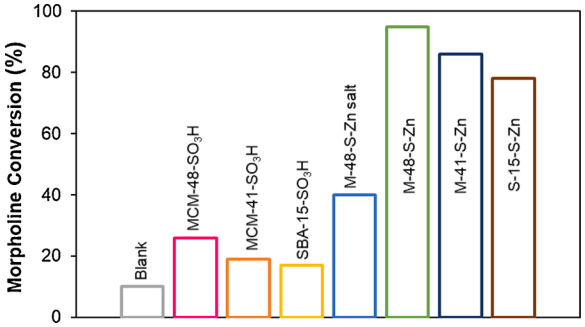

Fig. 6. Comparison of various catalysts in epoxide ring opening reaction. Reaction conditions: temperature, 70 °C; catalyst, 20 mg; time, 6 h; propylene oxide, 10 mmol; morpholine, 10 mmol.

may have more accessibility to the active sites hence maximum amount of Zn was anchored to the internal and external pore surfaces of MCM-48. We can correlate these data with the N_2 adsorption isotherm of M-48-S-Zn material. As the loading of Zn complex is maximum in MCM-48 material, the uniformity of the pore structure is somewhat disturbed, which is clearly reflected in the decrease of steepness of the curve in the range of p/p_0 0.2 to 0.8 in the material than the other two.

In order to confirm the linkage of Zn complex to the sulfopropylsilylated mesoporous silica materials, FT-IR spectra of pure Zn complex and Zn complex incorporated mesoporous materials were compared and shown in Fig. 5 A. All the materials exhibit broad bands at 787 and 1050 cm^{-1}attributed to Si–O–Si bending and stretching vibrations as well as silanolic OH groups [61,82] respectively. At 1390 cm^{-1} deformation vibration band of $-CH_2$ are also found for all the materials, which is ascribed from the propyl group linked to silanolic OH group due to presence of sulfonic acid group in the materials. Symmetric vibration of $–SO_3H$ groups as well as asymmetric vibration of S═O is found around 1000–1200 cm^{-1} wave length range respectively, but due to overlay with the Si–O–Si band at 1050–1150 cm^{-1} this peak cannot be separated. The IR spectrum of pure Zn complex displayed band at 1530 cm^{-1} due to C═N stretching vibration and the peak at 1450 cm^{-1} correspond to carbon-carbon stretching vibration of the aromatic rings. The Zn—O stretching frequency is observed at 720 cm^{-1}.

The acid concentration of prepared materials due to incorporation of Zn complex was calculated from NH_3-TPD measurements and NH_3-TPD profile is depicted in Fig. 5 B. As shown in Table 2, the total acidity of prepared materials was calculated and estimated by quantity of ammonia adsorbed. Total acid concentration was calculated from the NH_3 peak above 350 °C which was derived from the physically adsorbed ammonia on the surface of mesoporous silica. Calculated acidity of M-48-S-Zn catalyst was 0.82 mmol/g which was higher with compare to other two catalysts as well as from sulfopropylsilylated mesoporous materials (0.61 mmol/g), and it was clearly reflected in the catalysis result (Section 4.2.), as M-48-S-Zn showed maximum catalytic activity than the other two. We have compared the activities with sulfopropylsilylated catalysts also with less acidity as revealed by TPD analyses and discussed in the later section. Additionally, to investigate the thermal stability of prepared material and to study the amount of catalyst loading, thermogravimetric analysis was performed. The results are depicted in Fig. S2. The small weight loss around 5% was observed below 150 °C which was due to the presence of physiosorbed water in all three materials. The other weight loss in the temperature range of 200–600 °C was assigned to the decomposition of covalently bonded Zn complex with sulfonic acid group with propyl linkage of mesoporous materials. In this temperature range, around 15–17% weight loss was observed for all three materials.

Comparison of various catalysts on epoxide ring opening reaction

The efficiency of proposed modification method can be clearly understood after evaluation of catalytic activities in epoxide ring opening reaction of propylene oxide with morpholine using sulfopropylsilylated catalysts, Zn complex incorporated catalysts and also in the absence of catalyst. Fig. 6 shows the comparison of various catalysts in epoxide ring opening reaction.

Without any catalyst the reaction showed only 10% conversion of the reactant, whereas there were not much differences in conversion with sulfopropylsilylated mesoporous materials (15–25 %) also. There was a drastic change of catalytic activities when Zn-complex modified sulfopropylsilylated hybrid materials were used as catalysts. 95% reactant conversion was achieved with M-48-S-Zn material whereas M-41-S-Zn and S-15-S-Zn showed 86 % and 78 % conversion respectively. For comparison, another hybrid material by using Zn-acetate salt, impregnated with MCM-48-SO_3H was also prepared. 40% morpholine conversion was found, which clearly indicates the significance of Zn complex impregnation instead of Zn acetate salt in sulfopropylsilylated

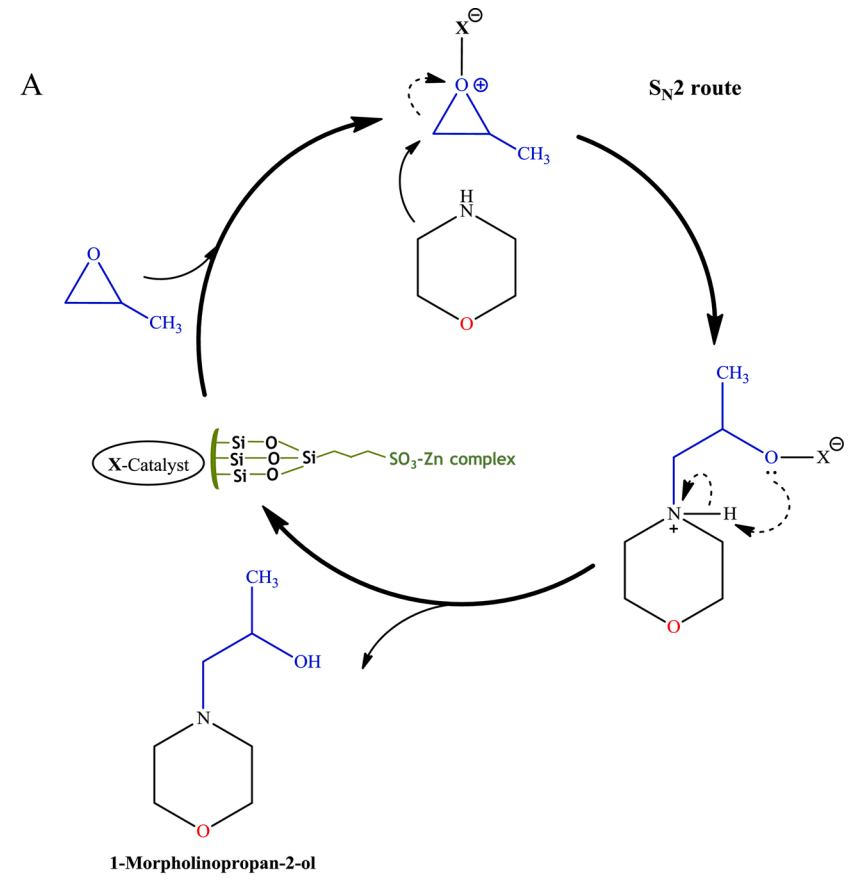

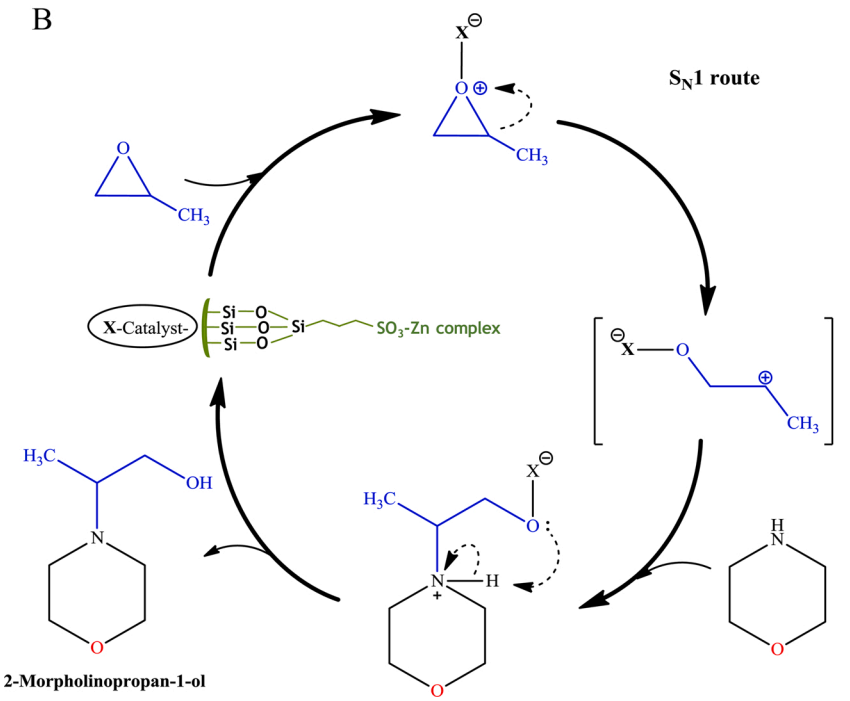

Scheme 5. **A.** A plausible mechanism of ring opening reaction of propylene oxide with moprholine via S_N2 route using Zn complex incorporated mesoporous silica as a catalyst [84]. **B.**

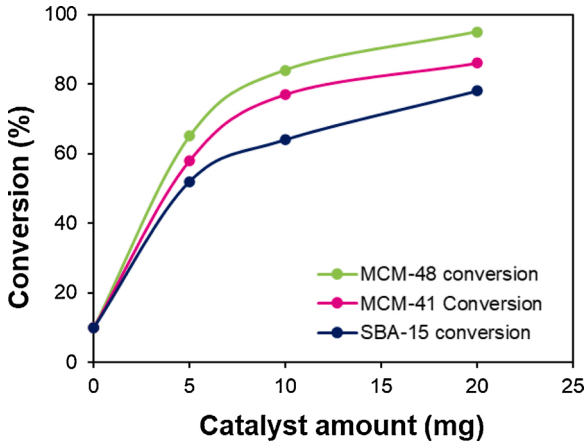

Fig. 7. Conversion of morpholine using different catalyst amount. Reaction conditions: temperature, 70 °C; time, 6 h; propylene oxide, 10 mmol; morpholine, 10 mmol.

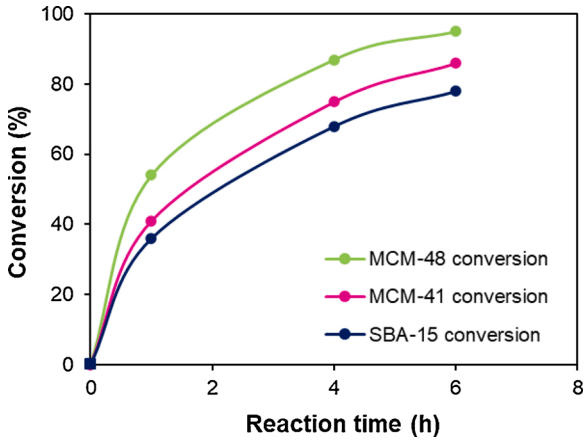

Fig. 8. Conversion of morpholine for different reaction time. Reaction conditions: temperature, 70 °C; catalyst, 20 mg; propylene oxide, 10 mmol; morpholine, 10 mmol.

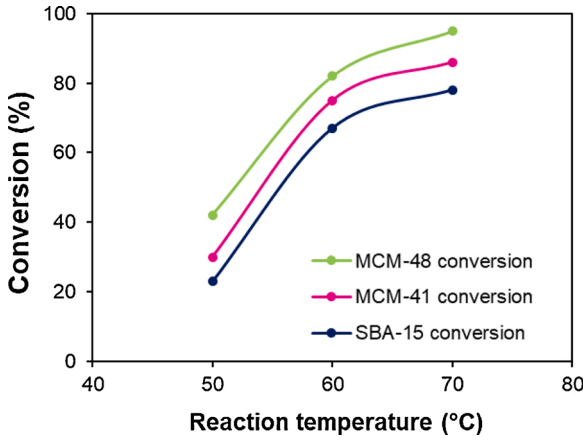

Fig. 9. Conversion of morpholine at different reaction temperatures. Reaction conditions: catalyst, 20 mg; time, 6 h; propylene oxide, 10 mmol; morpholine, 10 mmol.

mesoporous siica materials. The reactivity of a hybrid material depends on the type of ligands attached with the available site of centre metal ion to fulfil the coordination no after forming the bond with siliceous materials [83]. Here Zn-complex anchored with functionalized mesoporous material plays the key role in determining the high activity.

Above results clearly demonstrate the importance of Zn complex immobilized (Lewis acid) catalysts over sulfopropylsilylated (Brönsted acid) catalysts in the proposed reaction system. In this reaction, we have only calculated reactant conversion and selectivity of the products was not calculated as we were unable to separate the products from the reaction mixture. The contribution of the two mechanism (S_N2 and S_N1) depends on substrate, steric restriction, and reaction conditions. In the case of SBA-15, the space inside the pore is too large to give steric restriction. The substrate in this work is propylene oxide, which means the substituent is methyl group. The methyl group has some ability to stabilize the adjacent carbenium ion, but phenyl group has stronger ability to do so and has more tendency to choose S_N1 mechanism. On the other hand, the tendency to choose S_N2 mechanism depends on the strength of nucleophile. Investigation of substituents and nucleophile is future work and at this stage we focused on the catalyst preparation and its ability to catalyse the ring-opening of propylene oxide as a primary investigation in this work. The Lewis acidic nature of Zn ion in the tetranuclear Zn complex plays a significant role in this reaction and are the active sites for this organic-inorganic hybrid mesoporous materials. In the proposed epoxide ring opening reaction, ring opening of propylene oxide in presence of prepared lewis acid catalyst occurs according to possible S_N1 and S_N2 mechanism which leads to the formation of regioisomer products. 1-Morpholinopropan-2-ol product was formed via S_N2 route while 2-morpholinopropan-1-ol product was obtained via S_N1 route. The plausible mechanism for this reaction is depicted in Scheme 5A and B.

Reaction optimization

In order to attain the maximum conversion of reactant, reaction was optimized by changing reaction parameters like catalyst amount, time temperature etc. and the effect of reaction conversion on catalyst amount is shown in Fig. 7. 50–65% conversion was achieved when only 5 mg of catalyst was used, the conversion was increased simultaneously as amount of catalyst was increased. M-48-S-Zn catalyst showed 95% conversion using 20 mg of catalyst whereas M-41-S-Zn and S-15-S-Zn catalysts showed 86 % and 78 % conversion respectively with same reaction conditions. Reaction was also made using 30 mg of catalyst but there was not much change in the activities compare to 20 mg of catalysts.

The intrinsic catalytic activities or turnover frequencies were also calculated based on the acidity estimated from the TPD analyses for all the catalysts to have an idea about the availability of active sites from the catalytic point of view. TOF is considered as the number of catalytic series per unit time, mainly depends on the catalyst, temperature, pressure, and concentration [85]. Turnover frequency (TOF) values are summarized in Table 2. To check the efficiency of prepared catalysts in the proposed reaction, it has been found that TOF values of all the hybrid materials decreased with increase of the catalyst amount from 5 mg to 20 mg as well as with increase of reactant conversion. All the materials are found to be proficient in the proposed reaction system and also showed higher TOF values. Maximum TOF values were obtained for S-15-S-Zn catalyst and M-41-S-Zn catalysts have comparable values, though, M-48-S-Zn has comparatively lower TOF values under same reaction condition. However, catalytic result implies the prominent activity of M-48-S-Zn catalyst in the proposed reaction system. This may be due to the reason that MCM-48 has 3D framework and so has more available active sites in its structure. Therefore, when Zn complex was anchored to the MCM-48 material, may be higher extent of Zn complex was covalently tethered to the surface with compare to MCM-41 and SBA-15 material. Also the higher acid concentration was observed in MCM-48 material which is in good agreement with the above mentioned reason. Acidity of the M-48-S-Zn catalyst was found to be higher compared to other two catalysts; however, the higher TOF and best conversion are not fully contributed by the acidity of the material, rather

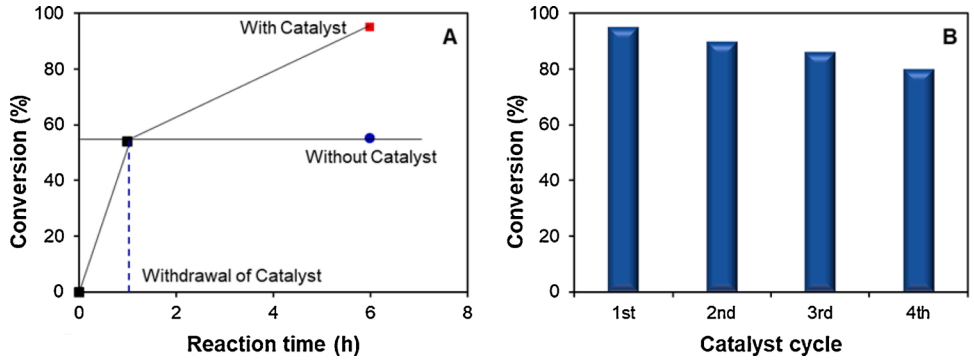

Fig. 10. (A) Heterogeneity test and (B) Recycle test of M-48-S-Zn catalyst. Reaction conditions: temperature, 70 °C; catalyst, 20 mg; time, 6 h; propylene oxide, 10 mmol; morpholine, 10 mmol.

other factors such as acid strength as well as framework structure have significant contribution towards the catalytic activity [86].

Reaction time is an important parameter to study the mechanism of reaction and so several reactions were performed for different durations to optimize reaction time. The catalytic performance of prepared catalysts displayed in Fig. 8 demonstrate that less amount of morpholine was converted into the product when reaction was performed for 1 h and it was increased rapidly as reaction time was increased up to 6 h. Morpholine conversion of all three catalyst proved that this reaction is time dependent and within 6 h of reaction time 95% morpholine conversion was achieved by M-48-S-Zn.

The effect of reaction temperature on the morpholine conversion was studied by varying reaction temperature and the results are summarized in Fig. 9. Reactions were performed for three different temperatures in order to achieve the maximum conversion of morpholine. Results indicate that, when the reactions were performed at 50 °C, morpholine conversion was less (40 % for M-48-S-Zn, around 20 % for M-41-S-Zn and S-15-S-Zn) for all three catalysts. As the temperature was increased to 60 °C, conversion of morpholine was also increased and on further increase in the temperature to 70 °C, 95 % morpholine conversion was found.

Heterogeneity of the catalyst

In order to check the heterogeneity of the prepared M-48-S-Zn catalyst two tests were performed, filtration test and recycle (Fig. 10). In the filtration test, Reaction was started at optimized conditions and after 1 h catalyst was removed from the reaction mixture by filtration and reaction was continued for further 5 h. As shown in the Fig. 10 A, there was no change in the conversion after removal of catalyst and after completion of the test (after 6 h) the morpholine conversion obtained was 55% which was well matched with the conversion on 1 h of reaction time (54%). Results clearly indicate the true heterogeneity of prepared M-48-S-Zn catalyst and confirm no leaching of active site into the reaction medium during the reaction path. Recycle test was also carried out to check the efficiency of prepared catalyst and it was performed for the M-48-S-Zn catalyst in the optimized reaction conditions. After each catalytic run, the catalyst was recovered by filtration, washed with acetone and dried at 80 °C. The catalyst was used for four catalytic cycles under the same reaction and regeneration conditions.

As shown in Fig. 10 B, no drastic change in morpholine conversion was observed and the catalytic activity was sustained even after 4th run with 80 % conversion over M-48-S-Zn catalyst. Slight gradual decrease in the conversion may be attributed to the deactivation of catalysts in successive runs which may have occurred due to the deposition of the product or substrate within the mesopore [60].

Conclusion

In this work, we have synthesized open cubane shaped Zn_4 complex utilizing multidentate Schiff base ligand which was further characterized by single crystal X-ray diffraction analysis. Later, this complex incorporated mesoporous silica materials were successfully prepared and anchoring of the complex was confirmed through thorough characterization techniques using powder XRD, N_2 adsorption/desorption analysis, SEM-EDX, FT-IR, NH_3-TPD, TGA and ICP-OES analysis. Mesoporous phase remains intact and homogeneous even after modification confirmed through powder XRD patterns. Successful immobilization of Zn complex to the sulfopropylsilylated mesoporous silica was confirmed by FT-IR spectroscopy, SEM-EDX, and ICP-OES analyses that showed the presence of Zn metal in the hybrid materials. The decrease in surface area, pore volume and pore diameter after modification was consistent with the presence of the organometallic complex inside the pore. The prepared catalysts, which were thoroughly characterized, were found to be highly active for ring opening reaction of propylene oxide with morpholine, and also noticeably M-48-S-Zn catalyst was found to be truly heterogeneous and reusable up to 4 times.

CRediT authorship contribution statement

Divya Jadav: Methodology, Writing - original draft. **Pooja Shukla:** Methodology. **Rajib Bandyopadhyay:** Visualization, Investigation. **Yoshihiro Kubota:** Characterization, Reviewing. **Sourav Das:** Conceptualization, Reviewing. **Mahuya Bandyopadhyay:** Conceptualization, Supervision, Reviewing, Editing.

Declaration of Competing Interest

The authors declare that they have no known competing financial interests or personal relationships that could have appeared to influence the work reported in this paper.

Acknowledgements

Divya Jadav and Pooja Shukla are thankful to IITRAM for providing financial support and infrastructural facilities. We would like to acknowledge IIT Gandhinagar for SEM-EDX analysis, and Mr. Kengo Takama of Yokohama National University for his technical assistance.

Appendix A. Supplementary data

Supplementary material related to this article can be found, in the online version, at doi:https://doi.org/10.1016/j.mcat.2020.111220.

References

[1] D.C. Sherington, in: B.K. Hodnett, A.P. Keybett, J.H. Clark, K. Smith (Eds.), Supported Reagents and Catalyst in Chemistry, Royal Society of Chemistry, Cambridge, 1998, pp. 220–228.
[2] K. Soai, M. Watanable, A. Yamamoto, J. Org. Chem. 55 (1990) 4832–4835, https://doi.org/10.1021/jo00303a014.
[3] T. Joseph, S.S. Deshpande, S.B. Halligudi, A. Vinu, S. Ernst, M. Hartmann, J. Mol. Catal. A Chem. 206 (2003) 13–21, https://doi.org/10.1016/S1381-1169(03)00452-7.
[4] T. Joseph, S.B. Halligudi, J. Mol. Catal. A Chem. 229 (2005) 241–247, https://doi.org/10.1016/j.molcata.2004.12.008.
[5] R. Sanyal, A. Guha, T. Ghosh, T. Kumar Mondal, E. Zangrando, D. Das, Inorg. Chem. 53 (2014) 85–96, https://doi.org/10.1021/ic4015493.
[6] A.K. Shivani, Chakraborti, J. Mol. Catal. A Chem. 263 (2007) 137–142, https://doi.org/10.1016/j.molcata.2006.08.047.
[7] G. Süss-Fink, M. Jahncke, in: R.D. Adams, F.A. Cotton (Eds.), Catalysis by Di- and Polynuclear Metal Cluster Complexes, Wiley-VCH, Toronto, ON, Canada, 1998.
[8] R.J. Puddephatt, in: P. Braunstein, L.A. Oro, P.R. Raithby (Eds.), Metal Clusters in Chemistry, Wiley-VCH, Toronto, ON, Canada, 1999.
[9] (a) G. Guillena, D.J. Ramon, M. Yus, in: M. Gupta, J.J. Spivey, Y.F. Han (Eds.), Asymmetric Organocatalyzed Morita-Baylis Hillman Reactions, Catalysis, Royal Society of Chemistry, UK, 2012, pp. 223–252;
(b) H.P. Mungse, S. Verma, N. Kumar, B. Sain, O.P. Khatri, J. Mater. Chem. 22 (2012) 5427–5433, https://doi.org/10.1039/C2JM15644J;
(c) A.E.C. Collis, I.T. Horvath, Catal. Sci. Technol. 1 (2011) 912–919, https://doi.org/10.1039/C1CY00174D;
(d) S. Verma, M. Nandi, A. Modak, S.L. Jain, A. Bhaumik, Adv. Synth. Catal. 353 (2011) 1897–1902, https://doi.org/10.1002/adsc.201100018;
(e) C. Pereira, J.F. Silva, A.M. Pereira, J.P. Araujo, G. Blanco, J.M. Pintado, C. Freire, Catal. Sci. Technol. 1 (2011) 784–793, https://doi.org/10.1039/C1CY00090J;
(f) J. Alauzun, A. Mehdi, C. Reye, R. Corriu, New J. Chem. 31 (2007) 911–915, https://doi.org/10.1039/B703155F.
[10] R. Luque, A.M. Balu, J.M. Campelo, M.D. Gracia, E. Losada, A. Pineda, A. A. Romero, J.C. Serrano-Ruiz, in: J.J. Spivey, M. Gupta, Y.-F. Han (Eds.), Catalysis, vol. 24, Royal Society of Chemistry, Cambridge, UK, 2012, pp. 253–280.
[11] C. Li, H. Zhang, D. Jiang, Q. Yang, Chem. Commun. 6 (2007) 547–558, https://doi.org/10.1039/B609862B.
[12] B. Liu, H. Liu, C. Wang, L. Liu, S. Wu, J. Guan, Q. Kan, Appl. Catal. A Gen. 443 (2012) 1–7, https://doi.org/10.1016/j.apcata.2012.06.020.
[13] Z. Li, L. Liu, J. Hu, H. Liu, S. Wu, Q. Huo, J. Guan, Q. Kan, Appl. Organometal. Chem. 26 (2012) 252–257, https://doi.org/10.1002/aoc.2861.
[14] M. Rimoldi, D. Fodor, J.A. van Bokhoven, A. Mezzetti, Chem. Commun. 49 (2013) 11314–11316, https://doi.org/10.1039/C3CC47296E.
[15] N. Canilho, J. Jacoby, A. Pasc, C. Carteret, F. Dupire, M.J. Stebe, J.L. Blin, Colloids Surf. B Biointerfaces 112 (2013) 139–145, https://doi.org/10.1016/j.colsurfb.2013.07.024.
[16] A.R. Massah, R.J. Kalbasi, S. Kaviyani, RSC Adv. 3 (2013) 12816–12825, https://doi.org/10.1039/C3RA22579H.
[17] B. Erdem, S. Erdem, R.M. Oksuzoglu, A. Citak, J. Porous Mater. 20 (2013) 1041–1049, https://doi.org/10.1007/s10934-013-9685-3.
[18] S. Alavi, H. Hosseini-Monfared, M. Siczek, J. Mol. Catal. A Chem. 377 (2013) 16–28, https://doi.org/10.1016/j.molcata.2013.04.013.
[19] Z. Ma, X. Wang, S. Wei, H. Yang, F. Zhang, P. Wang, J. Ma, Catal. Commun. 39 (2013) 24–29, https://doi.org/10.1016/j.catcom.2013.04.012.
[20] S. Sharma, B. Kerler, B. Subramaniam, A.S. Borovik, Green Chem. 8 (2006) 972–977, https://doi.org/10.1039/B602965E.
[21] X. Yang, J. Liu, Q. Kan, J. Guan, Polish J. Chem. Technol. 16 (2014) 12–17, https://doi.org/10.2478/pjct-2014-0043.
[22] P. Gellin, C. Naccache, Y.B. Taarit, Pure Appl. Chem. 60 (1988) 1315–1320, https://doi.org/10.1351/pac198860081315.
[23] P.A. Jacobs, R. Chantillon, P. DeLaet, J. Verdonck, M. Tielen, ACS Symp. Series 218 (1983) 439–453.
[24] A. Auroux, V. Bolis, P. Wierzchowski, P.C. Grzvelle, J.C. Vedrine, J. Chem. Soc. Faraday Trans. 1 (1979) 2544–2555, https://doi.org/10.1039/F19797502544.
[25] M. Iwamoto, H. Kusano, S. Kagawa, Inorg. Chem. 22 (1983) 3365–3366, https://doi.org/10.1021/ic00165a001.
[26] E. Mantovani, N. Palladino, A. Zanobi, J. Mol. Catal. 3 (1978) 285–291, https://doi.org/10.1016/0304-5102(78)80035-2.
[27] M.R. Maurya, M. Bisht, A. Kumar, M.L. Kuznetsov, F. Avecilla, J.C. Pessoa, Dalton Trans. 40 (2011) 6968–6983, https://doi.org/10.1039/C1DT10261C.
[28] M.R. Maurya, A.K. Chandrakar, S. Chand, J. Mol. Catal. A Chem. 274 (2007) 192–201, https://doi.org/10.1016/j.molcata.2007.05.018.
[29] A. Syamal, K.S. Kale, Indian J. Chem. 19A (1980) 225–228.
[30] A. Syamal, K.S. Kale, Indian J. Chem. 20A (1981) 205–208.
[31] C. Ratnasamy, A. Murugkar, S. Padhya, Indian J. Chem. 35A (1996) 1–3. http://nopr.niscair.res.in/handle/123456789/41239.
[32] S. Parihar, S. Pathan, R.N. Jadeja, A. Patel, V.K. Gupta, Inorg. Chem. 51 (2012) 1152–1161, https://doi.org/10.1021/ic202396q.
[33] S. Jana, B. Dutta, R. Bera, S. Koner, Langmuir 23 (2007) 2492–2496, https://doi.org/10.1021/la062409t.
[34] M. Alessandra, M. Andrea, B. Amra, G. Magnacca, Catal. Today 161 (2011) 64–69, https://doi.org/10.1016/j.cattod.2010.09.004.
[35] M. Pirouzmand, M.M. Amini, N. Safari, T. Hamoule, J. Braz. Chem. Soc. 24 (2013) 1864–1870, https://doi.org/10.5935/0103-5053.20130233.
[36] K. Plucinska, F. Kasprzykowski, E. Kozian, Tetrahedron Lett. 38 (1997) 861–864, https://doi.org/10.1016/S0040-4039(96)02426-4.
[37] M. Bolli, S. Ley, J. Chem. Soc. Perkin Trans. 1 (1998) 2243–2246, https://doi.org/10.1039/A803612H.
[38] A.K. Ghosh, Y. Wang, J. Org. Chem. 64 (1999) 2789–2795, https://doi.org/10.1021/jo9822378.
[39] E.J. Corey, F.Y. Zhang, Angew. Chem. Int. Ed. 38 (1999) 1931–1934, https://doi.org/10.1002/(SICI)1521-3773(19990712)38:13/14%3C1931::AID-ANIE1931%3E3.0.CO;2-4.
[40] P. O'Brien, Angew. Chem. Int. Ed. 38 (1999) 326–329, https://doi.org/10.1002/(SICI)1521-3773(19990201)38:3%3C326::AID-ANIE326%3E3.0.CO;2-T.
[41] D.J. Ager, I. Prakash, D.R. Schaad, Chem. Rev. 96 (1996) 835–876, https://doi.org/10.1021/cr9500038.
[42] E. Fullam, A. Abuhammad, D.L. Wilson, M.C. Anderton, S.G. Davies, A.J. Russell, E. Sim, Bioorg. Med. Chem. Let. 21 (2011) 1185–1190, https://doi.org/10.1016/j.bmcl.2010.12.099.
[43] R.M. Hanson, Chem. Rev. 91 (1991) 437–475, https://doi.org/10.1021/cr00004a001.
[44] A. Kamal, B.R. Prasad, A.M. Reddy, M.N. Khan, Catal. Commun. 8 (2007) 1876–1880, https://doi.org/10.1016/j.catcom.2007.02.029.
[45] D. Bhuyan, L. Saikia, D.K. Dutta, Appl. Catal. A Gen. 487 (2014) 195–201, https://doi.org/10.1016/j.apcata.2014.09.020.
[46] I. Matos, P.D. Neves, J.E. Castanheiro, E. Perez-Mayoral, R. Martin-Aranda, C. Duran-Valle, J. Vital, A.M. Botelho do Rego, I.M. Fonseca, Appl. Catal. A Gen. 439 (2012) 24–30, https://doi.org/10.1016/j.apcata.2012.06.036.
[47] J.S. Yadav, B.V. Reddy, A.K. Basak, A.V. Narsaiah, Tetrahedron Lett. 44 (2003) 1047–1050, https://doi.org/10.1016/S0040-4039(02)02735-1.
[48] J. Iqbal, A. Pandey, Tetrahedron Lett. 31 (1990) 575–576, https://doi.org/10.1016/0040-4039(90)87039-3.
[49] S. Ishida, S. Suzuki, T. Hayano, H. Furuno, J. Inanaga, J. Alloys. Compd. 408 (2006) 441–443, https://doi.org/10.1016/j.jallcom.2004.12.079.
[50] M.W. Robinson, A.M. Davies, I. Mabbett, T.E. Davies, D.C. Apperley, S.H. Taylor, A. E. Graham, J. Mol. Catal. A Chem. 329 (2010) 57–63, https://doi.org/10.1016/j.molcata.2010.06.018.
[51] N. Deshpande, A. Parulkar, R. Joshi, B. Diep, A. Kulkarni, N.A. Brunelli, J. Catal. 370 (2019) 46–54, https://doi.org/10.1016/j.jcat.2018.11.038.
[52] A.T. Placzek, J.L. Donelson, R. Trivedi, R.A. Gibbs, S.K. De, Tetrahedron Lett. 46 (2005) 9029–9034, https://doi.org/10.1016/j.tetlet.2005.10.106.
[53] H.F. Lu, J.T. Zhou, H.L. Cheng, L.L. Sun, F.F. Yang, R.Z. Wu, Y.H. Gao, Z.B. Luo, Tetrahedron 69 (2013) 11174–11184, https://doi.org/10.1016/j.tet.2013.10.098.
[54] T. Baskaran, A. Joshi, G. Kamalakar, A. Sakthivel, Appl. Catal. A Gen. 524 (2016) 50–55, https://doi.org/10.1016/j.apcata.2016.05.029.
[55] L. Xu, G. Fang, Y. Yu, Y. Ma, Z. Ye, Z. Li, Mol. Catal. 467 (2019) 1–8, https://doi.org/10.1016/j.mcat.2019.01.021.
[56] S. Roy, B. Banerjee, N. Salam, A. Bhaumik, S.M. Islam, ChemCatChem 7 (2015) 2689–2697, https://doi.org/10.1002/cctc.201500563.
[57] N. Nagarjun, P. Concepcion, A. Dhakshinamoorthy, Mol. Catal. 482 (2020) 110628, https://doi.org/10.1016/j.mcat.2019.110628.
[58] E. Cano-Serrano, G. Blanco-Brieva, J.M. Campos-Martin, J.L.G. Fierro, Langmuir 19 (2003) 7621–7627, https://doi.org/10.1021/la034520u.
[59] P.F. Siril, A.D. Davison, J.K. Randhawa, D.R. Brown, J. Mol. Catal. A Chem. 267 (2007) 72–78, https://doi.org/10.1016/j.molcata.2006.11.022.
[60] M. Bandyopadhyay, N. Tsunoji, T. Sano, Catal. Lett. 147 (2017) 1040–1050, https://doi.org/10.1007/s10562-017-1997-5.
[61] M. Bandyopadhyay, N. Tsunoji, R. Bandyopadhyay, T. Sano, React. Kinet. Mech. Catal. 126 (2019) 167–179, https://doi.org/10.1007/s11144-018-1447-4.
[62] P. Shukla, S. Roy, D. Dolui, W.C. Mancisidor, S. Das, Eur. J. Inorg. Chem. 2020 (2020) 823–832, https://doi.org/10.1002/ejic.201901350.
[63] M. Niwa, N. Katada, Catal. Surv. Jpn. 1 (1997) 215–226, https://doi.org/10.1023/A:1019033115091.
[64] SMART & SAINT Software Reference manuals, Version 6.45, Bruker Analytical X-ray Systems, Inc., Madison, WI, 2003.
[65] G.M. Sheldrick, SADABS, A Software for Empirical Absorption Correction, Ver. 2.05, University of Göttingen, Göttingen, Germany, 2002.
[66] SHELXTL, Reference Manual, Ver. 6.1, Bruker Analytical X-ray Systems, Inc., Madison, WI, 2000.
[67] G.M. Sheldrick, Acta Crystallogr. Sect. A: Found. Crystallogr. 64 (2008) 112–122.
[68] O.V. Dolomanov, L.J. Bourhis, R.J. Gildea, J.A.K. Howard, H. Puschmann, J. Appl. Crystallogr. 42 (2009) 339–341, https://doi.org/10.1107/S0021889808042726.
[69] K. Bradenburg, Diamond, Ver. 3.1eM, Crystal Impact GbR, Bonn, Germany, 2005.
[70] A.L. Spek, Acta Crystallogr. Sect. A 46 (1990) c34, https://doi.org/10.1107/S0108767390099780.
[71] G.A. Bain, J.F. Berry, J. Chem. Educ. 85 (2008) 532–536, https://doi.org/10.1021/ed085p532.
[72] A.W. Addison, T.N. Rao, J. Reedijk, J. Van Rijn, G.C. Verschoor, J. Chem. Soc. Dalton Trans. 7 (1984) 1349–1356, https://doi.org/10.1039/DT9840001349.
[73] S.K. Patel, R.N. Patel, Y. Singh, Y.P. Singh, D. Kumhar, R.N. Jadeja, H. Roy, A. K. Patel, N. Patel, N. Patel, A. Banerjee, D. Choquesillo-Lazarte, A. Gutierre, Polyhedron 161 (2019) 198–212, https://doi.org/10.1016/j.poly.2019.01.006.
[74] S. Ghosh, A. Spannenberg, E. Mejía, Helv. Chim. Acta 100 (2017) e1700176, https://doi.org/10.1002/hlca.201700176.
[75] B. Marler, U. Oberhagemann, S. Vortmann, H. Gies, Microporous Mesoporous Mater. 6 (1996) 375–383, https://doi.org/10.1016/0927-6513(96)00016-8.
[76] Q. Zhu, S. Maeno, R. Nishimoto, T. Miyamoto, M. Fukushima, J. Mol. Catal. A Chem. 385 (2014) 31–37, https://doi.org/10.1016/j.molcata.2014.01.013.

[77] S. Alavi, H. Hosseini-Monfared, M. Siczek, J. Mol. Catal. A Chem. 377 (2013) 16–28, https://doi.org/10.1016/j.molcata.2013.04.013.
[78] E. Sujandi, E.A. Prasetyanto, S.-C. Lee, S.-E. Park, Microporous Mesoporous Mater. 118 (2009) 134–142, https://doi.org/10.1016/j.micromeso.2008.08.035.
[79] J.-Q. Wang, L. Huang, M. Xue, Y. Wang, L. Gao, J.H. Zhu, Z. Zou, J. Phys. Chem. C 112 (2008) 5014–5022, https://doi.org/10.1021/jp7099948.
[80] M.J. Nasab, A.R. Kiasat, RSC Adv. 5 (2015) 75491–75499, https://doi.org/10.1039/C5RA11006H.
[81] V.H.A. Pinto, J.S. Rebouças, G.M. Ucoski, E.H. de Faria, B.F. Ferreira, R.A.S. San Gil, S. Nakagaki, Appl. Catal. A Gen. 526 (2016) 9–20, https://doi.org/10.1016/j.apcata.2016.07.018.
[82] Y. Li, G. Zhou, C. Li, D. Qin, W. Qiao, B. Chu, Colloids Surf. A Physicochem. Eng. Asp. 341 (2009) 79–85, https://doi.org/10.1016/j.colsurfa.2009.03.041.
[83] T. Das, H. Uyama, M. Nandi, J. Solid State Chem. 260 (2018) 132–141, https://doi.org/10.1016/j.jssc.2018.01.027.
[84] B. Shivani, A.K. Pujala, Chakraborti, J. Org. Chem. 72 (2007) 3713–3722, https://doi.org/10.1021/jo062674j.
[85] M. Boudart, Chem. Rev. 95 (1995) 661–666, https://doi.org/10.1021/cr00035a009.
[86] M. Kotwal, A. Kumar, S. Darbha, J. Mol. Catal. A Chem. 377 (2013) 65–73, https://doi.org/10.1016/j.molcata.2013.04.029.